

MuLan: Multimodal-LLM Agent for Progressive Multi-Object Diffusion

Sen Li¹ Ruochen Wang² Cho-Jui Hsieh² Minhao Cheng³ Tianyi Zhou⁴

Abstract

Existing text-to-image models still struggle to generate images of multiple objects, especially in handling their spatial positions, relative sizes, overlapping, and attribute bindings. In this paper, we develop a training-free **Multimodal-LLM agent** (MuLan) to address these challenges by progressive multi-object generation with planning and feedback control, like a human painter. MuLan harnesses a large language model (LLM) to decompose a prompt to a sequence of sub-tasks, each generating only one object conditioned on previously generated objects by stable diffusion. Unlike existing LLM-grounded methods, MuLan only produces a high-level plan at the beginning while the exact size and location of each object are determined by an LLM and attention guidance upon each sub-task. Moreover, MuLan adopts a vision-language model (VLM) to provide feedback to the image generated in each sub-task and control the diffusion model to re-generate the image if it violates the original prompt. Hence, each model in every step of MuLan only needs to address an easy sub-task it is specialized for. We collect 200 prompts containing multi-objects with spatial relationships and attribute bindings from different benchmarks to evaluate MuLan. The results demonstrate the superiority of MuLan in generating multiple objects over baselines. The code is available on <https://github.com/measure-infinity/mulan-code>.

1. Introduction

Diffusion models (Sohl-Dickstein et al., 2015; Ho et al., 2020; Song et al., 2020) have shown growing potential

¹Department of Computer Science and Engineering, The Hong Kong University of Science and Technology, Hong Kong, China

²Department of Computer Science, University of California, Los Angeles, USA

³College of Information Science and Technology, Penn State University, UAS

⁴Department of Computer Science, University of Maryland, College Park, USA. Correspondence to: Tianyi Zhou <tianyi@umd.edu>.

in generative AI tasks, especially in creating diverse and high-quality images with text prompts (Saharia et al., 2022; Rombach et al., 2022). However, current state-of-the-art text-to-image (T2I) models such as Stable Diffusion (Rombach et al., 2022) and DALL-E 3 (Betker et al., 2023) still struggle to deal with complicated prompts involving multiple objects and lack precise control of their spatial relations, potential occlusions, relative sizes, etc. As shown in Figure 2, to generate a sketch of “The orange pumpkin is on the right side of the black door”, even the SOTA open-source T2I model, Stable Diffusion XL (Podell et al., 2023), still generates wrong attribute-binding as well as incorrect spatial positions of several objects.

Among works that aim to improve the controllability of T2I models on complicated prompts, a recent promising line of research seeks to utilize large language models (LLMs), e.g., ChatGPT, GPT-4 (Achiam et al., 2023), to guide the generation process (Lian et al., 2023; Feng et al., 2023). Specifically, an LLM is prompted to generate a layout for the given prompt, i.e., a bounding box for each object in the image, given detailed instructions or demonstrations if necessary. However, due to the limited spatial reasoning capability of LLMs as well as their lack of alignment with the diffusion models, it is still challenging for LLMs to directly generate a complete and precise layout for multiple objects. Without a feedback loop interacting with the generative process, the layout’s possible mistakes cannot be effectively detected and corrected. Moreover, the layout is often applied as an extra condition in addition to the original prompt (e.g., bounding boxes combined with GLIGEN (Li et al., 2023)), so the diffusion models may still generate an incorrect image due to its misunderstanding of the complicated prompt.

To address the limitations and challenges of previous methods, we develop a training-free and controllable T2I generation paradigm that does not require demonstrations but mainly focuses on improving the tool usage of existing models. Our paradigm is built upon a progressive multi-object generation by a Multimodal-LLM agent (MuLan), which generates only one object per stage, conditioned on generated objects in the image and attention masks of the most plausible positions to place the new object. Unlike previous methods that add conditions to each model and make the task even more challenging, MuLan uses an LLM as a planner decomposing the original T2I task into a sequence

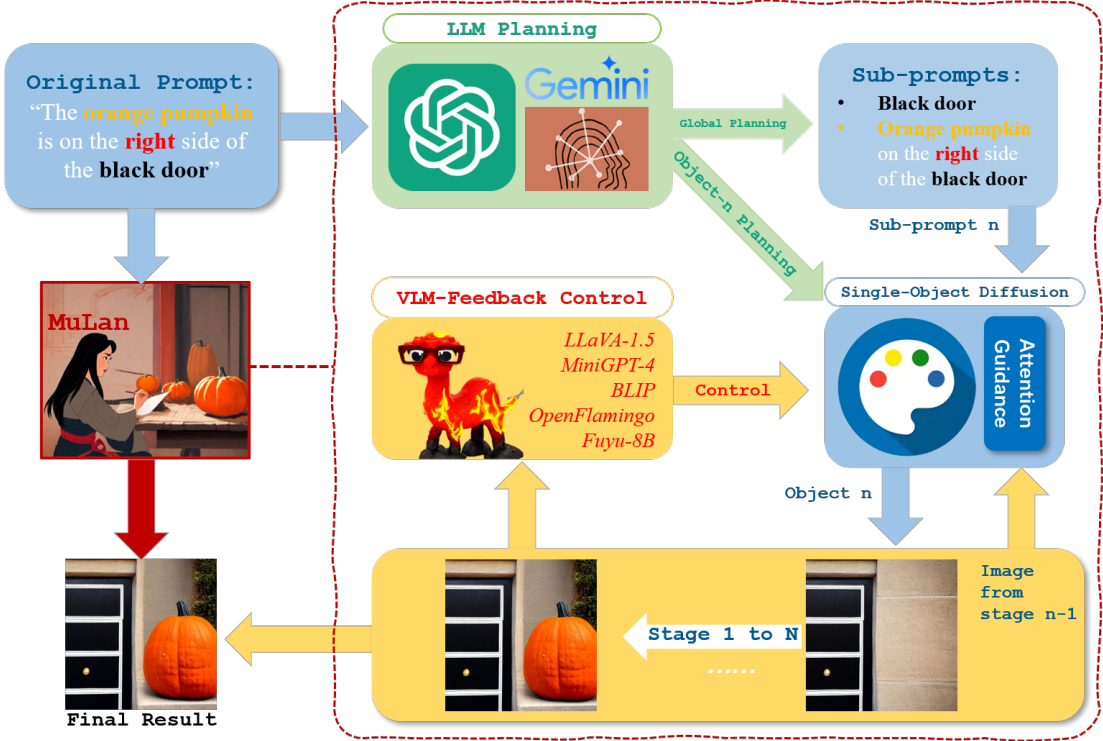


Figure 1. The proposed training-free Multimodal-LLM Agent (MuLan) for Progressive Multi-Object Diffusion. MuLan consists of three main components: (1) LLM planning; (2) Single-object diffusion with attention guidance; and (3) VLM-feedback control. MuLan first decomposes a complicated prompt into a sequence of sub-prompts each for one object, and then generates one object per step conditioned on a sub-prompt and previously generated objects, where LLM plans the rough layout of the object and attention guidance provides an accurate mask for it. The VLM-feedback control allows MuLan to correct mistakes in each step by adjusting hyperparameters in (2).

of easier subtasks. Each subtask generates one single object, which can be easily handled by diffusion models. To be noted, the LLM applied at the beginning of MuLan only focuses on high-level planning rather than a precise layout of bounding boxes, while the exact size and position of each object are determined later in each stage by LLM and attention guidance based on the generated objects in the image. Hence, we can avoid mistakes in the planning stage and find a better placement for each object adaptive to the generated content and adhering to the original prompt. In addition, MuLan builds a feedback loop monitoring the generation process, which assesses the generated image per stage using a vision-language model (VLM). When the generated image violates the prompt, the VLM will adjust the diffusion model to re-generate the image so any mistake can be corrected before moving to the next stage. Furthermore, we develop a strategy applied in each stage to handle the overlapping between objects, which is commonly ignored by previous work (Lian et al., 2023).

Therefore, MuLan obtains better controllability of the multi-object composition. An illustration of the progressive generation process is shown in Figure 1. To evaluate MuLan, we curate a dataset of intricate and challenging prompts from

different benchmarks. To compare MuLan with existing approaches, we prompt GPT-4V (OpenAI, 2023) several questions based on the input texts to comprehensively evaluate the alignment of the generated images with the prompts from three aspects. We further conduct human evaluations of the generated images. Extensive experimental results show that MuLan can achieve better controllability over the generation process and generate high-quality images aligning better with the prompts than the baselines. Example images generated by different methods are shown in Figure 2. Our main contributions are summarized as follows:

- We propose a novel training-free paradigm for text-to-image generation and a Multimodal-LLM agent. It achieves better control in generating images for complicated prompts consisting of multiple objects with specified spatial relationships and attribute bindings.
- We propose an effective strategy to handle multi-object occlusion in T2I generation, which improves the image quality and makes them more realistic.
- We curate a dataset of prompts to evaluate multi-object composition with spatial relationships and attribute bindings in T2I tasks. The quantitative results and human

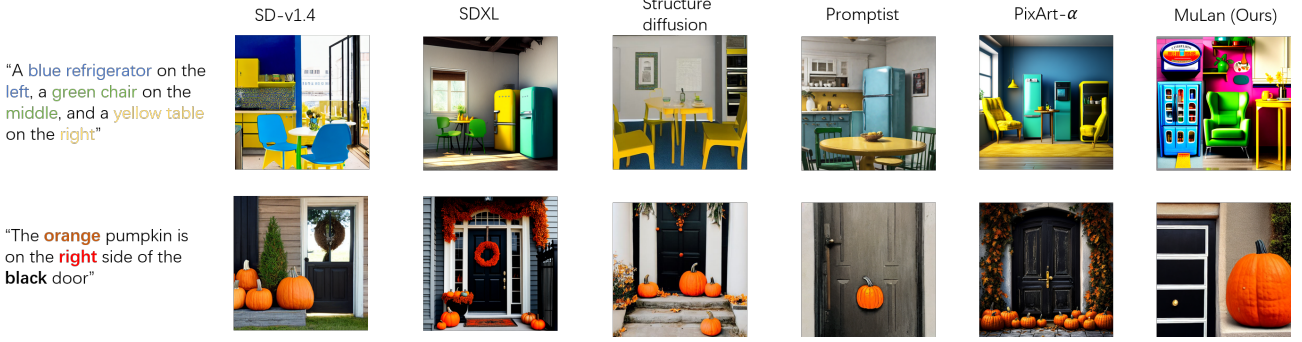


Figure 2. Examples of MuLan-generated images, compared to the original SD-v1.4 (Rombach et al., 2022), the original SDXL (Podell et al., 2023), Structure diffusion (Feng et al., 2022), Promptist (Hao et al., 2022), and PixArt- α (Chen et al., 2023).

evaluation results show that our method can achieve better results compared to different controllable generation methods and general T2I generation methods.

2. Related Work

Diffusion models As a new family of generative models, diffusion models have attracting more and more attention due to its powerful creative capability. Text-to-image generation, which aims to generate the high-quality image aligning with given text prompts, is one of the most popular applications (Nichol et al., 2021; Saharia et al., 2022; Rombach et al., 2022; Betker et al., 2023). Among different powerful diffusion models, the latent diffusion model (Rombach et al., 2022) has shown amazing capability and has been widely used in practice due to the efficiency and superior performance, which is also the backbone of the current SOTA stable diffusion models. Different from the typical diffusion models which directly perform the diffusion and denoising process in the pixel space, the latent diffusion model perform the whole process in the encoded latent space (Rombach et al., 2022), which can greatly reduce the training and inference time. Recently, empowered by a significantly expanded model capacity, Stable Diffusion XL has demonstrated performance levels approaching commercial application standards (Podell et al., 2023).

Composed generation in diffusion models Although Stable Diffusion model has shown unprecedented performance on the T2I generation task, it still struggles with text prompts with multi-object, especially when there are several spatial relationships and attribute bindings in the prompts. To achieve more controllable and accurate image compositions, many compositional generation methods have been proposed. StructureDiffusion (Feng et al., 2022) proposed a training-free method to parse the input prompt and combine it with the cross-attention to achieve better control over attribute bindings and compositional generation. On the other hand, Promptist (Hao et al., 2022) aimed to train a language model with the objective of optimizing input prompts, rendering them more comprehensible and facilitative for

diffusion models. Recently, several works utilize the large language model to directly generate the whole layout for the input prompt with in-context learning, and then generate the image conditioned on the layout (Lian et al., 2023; Feng et al., 2023). While all the previous take the whole input prompt, we propose to turn the original complicated task into several easier sub-tasks. A training-free multimodal-LLM agent is utilized to progressively generate objects with feedback control so that the whole generation process would be better controlled.

3. Multimodal-LLM Agent (MuLan)

Existing diffusion models often struggle with complicated prompts but can handle simpler ones. Recent approaches train a model or apply in-context learning given similar examples to produce a detailed layout for the prompt in advance and the diffusion model can generate each part of the layout with a simpler prompt separately. Rather than generating all objects at once or in parallel, MuLan is inspired by many human painters, who start by making a high-level plan, painting objects one after another as planned, and correcting mistakes after each step if needed. Thereby, the constraints between objects can be naturally taken into account.

3.1. Problem Formulation

Likewise, MuLan begins by strategically planning and decomposing an intricate input prompt into a manageable sequence of sub-prompts, each focusing on an easier sub-task generating one single object. MuLan then adopts a progressive strategy that generates one object in each stage conditioned on previously generated objects using a diffusion model. Simultaneously, a VLM offers insightful feedback and adaptively adjusts the generation process to guarantee precision in accomplishing each subtask. Compared to previous methods, MuLan is entirely training-free and does not require any examples. As illustrated in Fig. 1, MuLan is composed of three components:

- **Prompt decomposition by LLM planning**, which produces a sequence of sub-prompts, each focusing on gener-

ating one object in the prompt.

- **Conditional single-object diffusion with LLM planning and attention guidance**, which generates a new object conditioned on the previous step’s image using a stable diffusion model. While a sub-prompt from LLM planning provides text guidance, the object’s size and position are controlled by an attention mask.
- **VLM-feedback control**, which inspects the image generated per stage and adjusts hyperparameters to re-generate the image if it violates the original prompt.

3.2. Background on (Latent) Diffusion Models

Consisting of the diffusion process and the reverse process, diffusion models have shown impressive capability for high-quality image generation by iteratively adding noise and denoising (Ho et al., 2020). Let $x_0 \sim q(x_0)$ be the true data distribution. Starting from x_0 , the diffusion process adds different levels of noise pre-defined by the schedule $\{\beta_t\}_1^T$, producing x_1, \dots, x_T . As $T \rightarrow \infty$, x_T will become the standard Gaussian distribution $\mathcal{N}(\mathbf{0}, \mathbf{I})$. Accordingly, the reverse process aims to reverse the above process and reconstruct the true data distribution from $p(x_T) = \mathcal{N}(\mathbf{0}, \mathbf{I})$ by a parameterized noise model $\epsilon_\theta(\cdot)$. With $\epsilon \sim \mathcal{N}(\mathbf{0}, \mathbf{I})$, the training loss of the model can be simplified as

$$L(\theta) = \mathbb{E}_{t, x_0, \epsilon} \|\epsilon - \epsilon_\theta(\sqrt{\bar{\alpha}_t} x_0 + \sqrt{1 - \bar{\alpha}_t} \epsilon, t)\|^2. \quad (1)$$

Latent diffusion models (Rombach et al., 2022) have recently attracted growing attention due to their efficiency and superior performance. Instead of performing diffusion and its reverse process in the pixel space, they add noise and denoise in a latent space of z encoded by a pre-trained encoder \mathcal{E} . Thereby, the diffusion process starts from $z_0 = \mathcal{E}(x_0)$ and subsequently produces latent states $z_1, \dots, z_t, \dots, z_T$. Accordingly, the training loss becomes

$$L_{LDM} = \mathbb{E}_{z_0, \epsilon, t} \|\epsilon - \epsilon_\theta(z_t, t)\|^2. \quad (2)$$

3.3. Prompt Decomposition by LLM Planning

Given a complicated prompt p , MuLan first uses an LLM to automatically decompose p into N object-wise sub-prompts $p_{1:N}$. MuLan specifically asks the LLM to produce a sequence of objects that will be created in the default order from left to right and bottom to top in the image, so the LLM leverages its prior knowledge to fill all objects of p to an empty list of the pre-defined order. Compared to layout generation, this is more feasible for most LLMs who may suffer from hallucinations in spatial reasoning. The pre-defined order will also facilitate sequential object generation in Section 3.4. Let $objs = \{obj_1, \dots, obj_n, \dots, obj_N\}$ be the LLM-planned N objects extracted from p . For the first object, the sub-prompt is simply $p_1 = \{"obj_1"\}$. For

object- n with $n > 1$, the subtask is to generate object- n conditioned on previous objects and the textual sub-prompt is defined as $p_n = \{"obj_n\}$ and $\{obj_{n-1}\}$. MuLan conducts the above global planning by an LLM at the very beginning before generating any image. The detailed prompts and template for LLM planning can be found in Appendix A.

When generating each object in Section 3.4, we will use the LLM again as a local planner of the object’s position and size, i.e., by generating a mask in the image and coordinating its overlap with previous objects. Then a diffusion model is used to generate the object under the attention guidance of the mask. These will be further elaborated in Section 3.4.

3.4. Conditional Single-Object Diffusion with LLM Planning and Attention Guidance

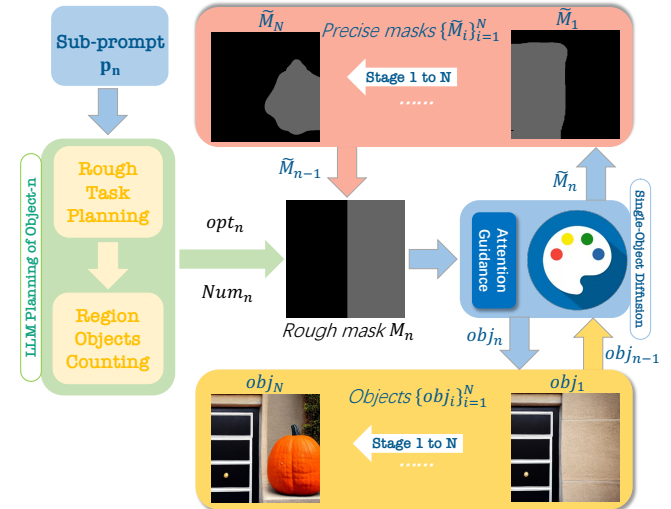


Figure 3. Single object diffusion with LLM planning and attention guidance for obj_n (detailed procedure in Algorithm 1).

At stage- n , the diffusion model only focuses on generating obj_n according to the sub-prompt p_n under attention guidance, which is based on a rough mask (i.e., a bounding box) M_n for obj_n . M_n is derived from obj_n ’s relative position and size planned by the LLM, conditioned on the current space availability in the image. When $n > 1$, M_n also depends on the previous object obj_{n-1} and its precise mask \tilde{M}_{n-1} in the image generated in stage-($n-1$). The pipeline is given in Figure 3 with the complete procedure listed in Algorithm 1. We will introduce it step by step in the following.

LLM Planning of a Rough Mask for obj_n . At stage- n , MuLan first derives a rough mask as a bounding box $M_n \triangleq (x_n, y_n, w_n, h_n)$ (x/y coordinates of the top-left corner, width, and height) for obj_n in the image. As shown in Figure 3, M_n can be derived from obj_n ’s rough position $opt_n \in \text{Opt}_{\text{S}} = \{\text{left}, \text{right}, \text{top}, \text{bottom}\}$, the total number of objects Num_n in the same position/region as obj_n , and the precise mask \tilde{M}_{n-1} of previously generated

Algorithm 1 Single Object Diffusion in MuLan

```

1: Input: Object number  $n$ , sub-prompt  $p_n$ , LLM planner
   Planner, precise mask  $\tilde{M}_{n-1}$  (only for  $n > 1$ ), latents
    $\{\mathbf{z}_{(n-1),(t-1)}\}_{t=1}^T$  (only for  $n > 1$ ), attention guidance
   timestep threshold  $T'$ , combination timestep threshold  $T^*$ 
   (only for  $n > 1$ ), diffusion model  $\mathcal{D}$ .
2: Output: Image with  $\text{obj}_n$  and its precise mask  $\tilde{M}_n$ .
3: if  $n = 1$  then
4:    $\text{opt}_1, \text{Num}_1 = \text{Planner}(p_1)$ 
5:   Apply Eq. (3) to compute  $M_1$ 
6:   for  $t = T, \dots, 1$  do
7:     if  $t > T'$  then
8:       Apply Eq. (6) with  $M_1$ 
9:     end if
10:     $\mathbf{z}_{1,(t-1)} = \mathcal{D}(\mathbf{z}_{1,t}, t, p_1)$  {Single denoising step}
11:   end for
12: else
13:    $\text{opt}_n, \text{Num}_n = \text{Planner}(p_n, \{\text{obj}_i\}_{i=1}^{n-1})$ 
14:   Apply Eq. (4) to compute  $M_n$ 
15:   for  $t = T, \dots, 1$  do
16:     if  $t > T'$  then
17:       Apply Eq. (6) with  $M_n$ 
18:     end if
19:      $\mathbf{z}_{n,(t-1)} = \mathcal{D}(\mathbf{z}_{n,t}, t, p_n)$ 
20:     if  $t > T^*$  then
21:       Apply Eq. (7) to combine latent of  $\text{obj}_n$  and  $\text{obj}_{n-1}$ 
22:     end if
23:   end for
24: end if
25:  $\text{obj}_n = \mathbf{z}_{n,0}$ 
26:  $\tilde{M}_n = (\tilde{x}_n, \tilde{y}_n, \tilde{w}_n, \tilde{h}_n)$ , a bounding box based on thresholding of  $\frac{1}{|B|} \sum_{j \in B} \mathbf{A}_{(:,k)}^{(j)}$  {Token- $k$  corresponds to  $\text{obj}_n$ }

```

obj_{n-1} . MuLan utilizes an LLM planner to determine opt_n and Num_n given the sub-prompt p_n ¹, while \tilde{M}_{n-1} can be easily derived from the generated image from stage- $(n-1)$ with opt_{n-1} .

When $n = 1$, since there is not any object generated yet, both the position opt_1 and Num_1 are unrestricted and the LLM can be prompted to determine opt_1 and Num_1 given sub-prompt p_1 . Since the object order starts from left to right and bottom to top, there will be only two position options $\text{opt}_1 \in \{\text{left}, \text{bottom}\}$ for obj_1 . Once opt_1 determined, as shown in Figure 5, MuLan evenly splits the whole image's width W (H) to Num_1 parts and assigns the very left (bottom) part to obj_1 , which leads to the following bounding box:

$$M_1 = \begin{cases} (0, 0, \frac{W}{\text{Num}_1}, H), & \text{opt}_1 = \text{left}, \\ (\frac{(\text{Num}_1-1) \cdot H}{\text{Num}_1}, 0, W, \frac{H}{\text{Num}_1}), & \text{opt}_1 = \text{bottom}. \end{cases} \quad (3)$$

When $n > 1$, the position opt_n denotes $\{\text{obj}\}_n$'s relational position to the previous object $\{\text{obj}\}_{n-1}$. Since MuLan generates objects from left to right and from bottom to top, $\text{opt}_n \in \{\text{right}, \text{top}\}$. Given sub-

¹The detailed prompt template can be found in Appendix B.

prompt p_n , an LLM is prompted to select opt_n and determine Num_n . Meanwhile, the precise mask $\tilde{M}_{n-1} = (\tilde{x}_{n-1}, \tilde{y}_{n-1}, \tilde{w}_{n-1}, \tilde{h}_{n-1})$ of opt_{n-1} can be extracted from the image with $\{\text{obj}\}_{n-1}$ generated (e.g., by text-image cross-attention maps in the diffusion model). Hence, the rough mask M_n for obj_n can be derived from opt_n , Num_n , and \tilde{M}_{n-1} as followings.

$$M_n = \begin{cases} (\tilde{x}_{n-1} + \tilde{w}_{n-1}, 0, \frac{W - \tilde{x}_{n-1} + \tilde{w}_{n-1}}{\text{Num}_n}, H), & \text{if } \text{opt}_n = \text{right}, \\ (0, \frac{\tilde{y}_{n-1} \cdot (\text{Num}_n - 1)}{\text{Num}_n}, W, \frac{\tilde{y}_{n-1}}{\text{Num}_n}), & \text{if } \text{opt}_n = \text{top}. \end{cases} \quad (4)$$

Figure 4 illustrates how the rough mask can be computed based on the precise mask of previous objects.

Single-Object Diffusion with Attention Guidance. Given the rough mask M_n of obj_n in the image, MuLan can precisely generate obj_n in the image using the backward guidance method (Chen et al., 2024), which guides the attention masks of the object to be positioned correctly during generation. Specifically, let B be the set of the blocks containing cross-attentions layers in the diffusion model, $\mathbf{A}^{(j)}$ be the cross-attention map in the j -th block, $j \in B$, $\mathbf{A}_{m,k}^{(j)}$ represents the relevance between the spatial location m and token- k that describes obj_n in the prompt, and $|\mathbf{A}_{(:,k)}^{(j)}| = W \cdot H$ is the cross-attention map of token k . Larger values in $\mathbf{A}_{m,k}^{(j)}$ indicate that obj_n is more likely located at the spatial location of m . Hence, minimizing the following energy function encourages the cross-attention maps to the k -th token (obj_n) to have a larger value inside the mask:

$$E(\mathbf{A}^{(j)}, M_n, k) = \left(1 - \frac{\sum_{m=x_n+(y_n-1)W}^{x_n+w_n+(y_n+h_n-1)W} \mathbf{A}_{m,k}^{(j)}}{\sum_{m=1}^{W \cdot H} \mathbf{A}_{m,k}^{(j)}} \right)^2. \quad (5)$$

Then, in every step- t of the earlier generation process ($t > T'$), MuLan applies gradient descent to minimize the energy and updates the input latent $\mathbf{z}_{n,t}$ for object obj_n by

$$\mathbf{z}_{n,t} = \mathbf{z}_{n,t} - \eta \cdot \nabla_{\mathbf{z}_{n,t}} \sum_{j \in B} E(\mathbf{A}^{(j)}, M_n, k), \quad (6)$$

where η is the learning rate. In practice, to take the previous objects and their constraints into account when generating obj_n , during earlier steps of backward diffusion (i.e., $t > T^*$), we further combine the latent of obj_n and obj_{n-1} . Specifically, after step- t of backward diffusion (t varies from T to 0), we update the latent $\mathbf{z}_{n,(t-1)}$ by

$$\mathbf{z}_{n,(t-1)} = \mathbf{M}'_n \odot \mathbf{z}_{n,(t-1)} + (1 - \mathbf{M}'_n) \odot \mathbf{z}_{(n-1),(t-1)}, \quad (7)$$

where \odot computes element-wise product and $[\mathbf{M}'_n]_{uv} = \mathbb{1}_{u \in [x_n, x_n + w_n], v \in [y_n, y_n + h_n]}$ is the 0-1 indicator of whether coordinates (u, v) is included in the bounding box of \mathbf{M}_n .

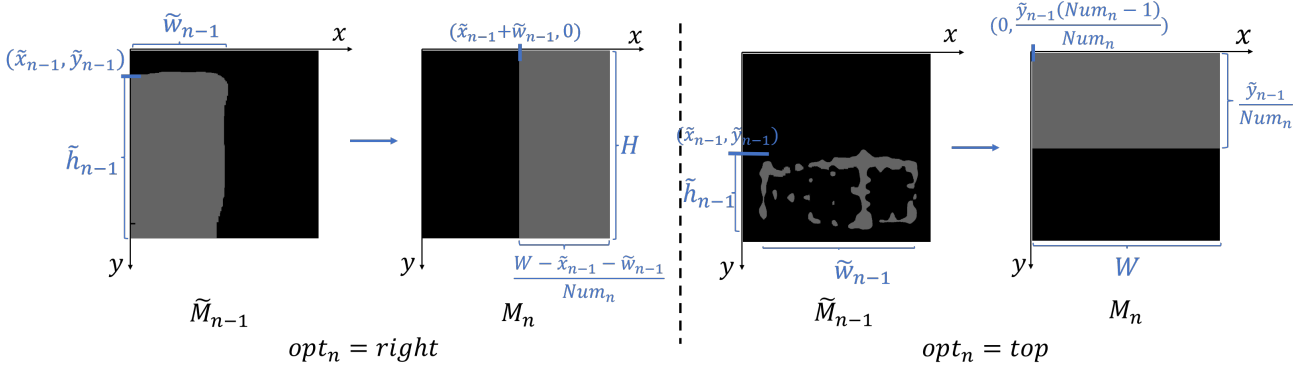


Figure 4. The rough mask M_n of $\text{obj}_n (n > 1)$ is derived from the precise mask \tilde{M}_{n-1} of the previously generated object obj_{n-1} .

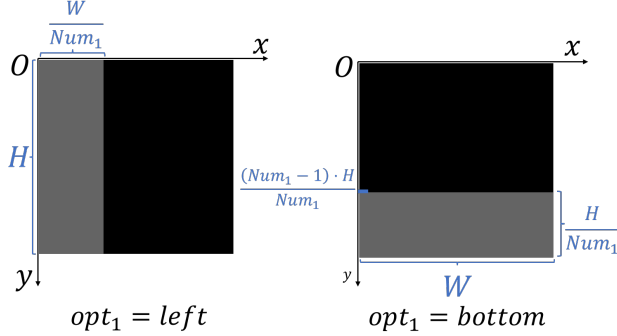


Figure 5. Illustration of the rough mask M_1 of obj_1 . There are only two options `left`, `bottom` for the mask since the LLM is prompted to plan the object order from left to right, bottom to top.

MuLan applies the above single-object diffusion to each object one after another from obj_1 to obj_N , as planned by the LLM at the very beginning. The procedure of generating obj_n is detailed in Algorithm 1. In each stage- n , MuLan applies an LLM planner to determine the location opt_n of obj_n and object count Num_n at opt_n . MuLan then derives a rough mask M_n from opt_n , Num_n , and previously generated object’s precise mask. Given M_n , MuLan applies a diffusion model to generate obj_n in the M_n -defined bounding box via attention guidance.

Overlapping between Objects Overlapping between objects is a key challenge when generating one object conditioned on the previous one(s). However, it lacks attention in previous methods (Lian et al., 2023; Feng et al., 2023). Instead, we propose an effective strategy that can be merged into the procedure above. Specifically, at the generation of object obj_n , we prompt the LLM to judge if there is overlapping between obj_n and obj_{n-1} . If there is no overlapping, the generation is the same as described above. If there is overlapping, we first compute three candidates for the rough mask $\{M_{n,i}\}_{i=1}^3$, associated with three overlapping ratios $\{r_i\}_{i=1}^3 = \{10\%, 30\%, 50\%\}$ between obj_{n-1} and obj_n . An illustration is given in Figure 7 with more details of candidate masks in Appendix C.

Given the three masks $M_{n,i}$, we generate three candidate images using Algoirthm 1. Then the CLIP scores (Hessel

et al., 2021) between the generated images and the input prompt p_n are computed and the image with the maximal CLIP score is selected as the generated image for obj_n .

3.5. Adaptive Feedback Control by VLM

To correct the possible mistakes made in the sequential generation process, MuLan builds a feedback-loop control by a vision-language model (VLM). After each generation stage, MuLan queries the VLM to inspect the generated object(s) and its consistency with the input prompt. If they do not align well, MuLan will adjust the backward guidance and T^* of the current stage to re-generate the object. Such a close-loop control involves LLM, diffusion, and VLM and significantly automates the T2I generation for complicated prompts, leading to a more accurate generation in practice.

4. Experiments

Dataset To evaluate our framework, we construct a prompt dataset from different benchmarks. Specifically, since our focus is to achieve better generation for complex prompts containing multi-objects with both spatial relationships and attribute bindings, we first collect all complex spatial prompts from T2I-CompBench (Huang et al., 2023). To make the experiments more comprehensive, we let ChatGPT generate about 400 prompts with different objects, spatial relationships, and attribute bindings so that the prompt sets consists of about 600 prompts. To further evaluate the capability of our framework on extremely complex and hard prompts, we manually add prompts that SDXL fails to generate, leading to a hard prompt dataset containing 200 prompts. Similar to the complex spatial prompts in T2I-CompBench (Huang et al., 2023), each prompt in our curated dataset typically contains two objects with various spatial relationships, with each object containing attribute bindings randomly selected from {color, shape, texture}.

Models & Baseline As a training-free framework, MuLan can be incorporated into any existing diffusion models. We evaluate two stable diffusion models with our framework,

Table 1. GPT-4V evaluation/human evaluation of images generated by different methods for complicated prompts.

| Method | Object completeness | Attribute bindings | Spatial relationships | Overall |
|---|-----------------------|-------------------------------|-------------------------------|-----------------------|
| Structure Diffusion (Feng et al., 2022) | 88.97%/87.37% | 54.62%/62.63% | 34.36%/24.24% | 64.31%/64.85% |
| Promptist-SD v1.4 (Hao et al., 2022) | 80.36%/70.71% | 49.23%/52.02% | 24.49%/13.13% | 56.73%/51.72% |
| Promptist-SDXL (Hao et al., 2022) | 94.36%/ 93.94% | 70.00%/78.28% | 35.89%/33.33% | 72.92%/75.56% |
| SD v1.4 (Rombach et al., 2022) | 90.31%/74.49% | 57.14%/51.02% | 37.24%/32.65% | 66.43%/56.73% |
| SDXL (Podell et al., 2023) | 94.64%/78.57% | 66.07%/53.06% | 41.14%/24.49% | 72.34%/57.55% |
| PixArt- α (Chen et al., 2023) | 92.09%/76.53% | 66.58%/61.22% | 34.69%/32.65% | 70.41%/61.63% |
| MuLan-SD v1.4 (Ours) | 93.11% /86.36% | 74.23%/74.24% | 51.53% / 54.54% | 77.24% /75.15% |
| MuLan-SDXL (Ours) | 96.17% /90.40% | 75.00% / 79.29% | 39.29%/49.49% | 76.33%/ 77.78% |

Stable Diffusion v1.4 (Rombach et al., 2022) and the SOTA Stable Diffusion XL (Podell et al., 2023). To verify the superiority of MuLan, we compare it with previous controllable generation methods and general T2I generation methods. Specifically, we evaluate Structure Diffusion (Feng et al., 2022), Promptist (Hao et al., 2022), the original Stable Diffusion v1.4, the original SDXL, and the recent SOTA diffusion model PixArt- α (Chen et al., 2023).

Implementation Details MuLan use GPT-4 (Achiam et al., 2023) as the LLM planner, and LLaVA-1.5 (Liu et al., 2023) as the VLM checker to provide the feedback. We also conducted an ablation study to show the importance of the feedback control provided by the VLM and the effect of different VLMs. Moreover, we found the attention blocks utilized during the attention guidance are vital, which can be classified as near-input blocks, near-middle blocks, and near-output blocks. We utilize the near-middle blocks in our main experiments and also show the ablation results of different blocks.

Evaluation Since the prompt dataset contains texts with complex compositions, we design a questionnaire to comprehensively investigate the alignment between the generated image and the corresponding input text. The questionnaire is composed of three aspects - object completeness, correctness of attribute bindings, and correctness of spatial relationships. We only set two options for each question (Yes or No), without any ambiguity. For detailed questions and examples of the evaluation, please refer to Appendix D. For each aspect of the evaluation, we compute the percentage of answers with “Yes”. Given the generated image, we assess the image’s quality using a questionnaire asking both the state-of-the-art multi-modal large language model (GPT-4V (OpenAI, 2023)) and the human evaluator.

4.1. Main Results and Analysis

Results with GPT Evaluation Given the generated image, we prompt GPT-4V to answer the questions about the image in the questionnaire, where each only focuses on one of the three aspects. The results for different methods and different base models are shown in Table 1. The results

show that our framework can achieve the best performance compared to different controllable generation methods and T2I generation methods. In particular, in the two ‘harder’ aspects - attribute bindings and spatial relationships, MuLan can surpass other methods by a large margin. More qualitative results can be found in Figure 6 and Appendix E.

Results with Human evaluation To further accurately evaluate the generated images about the alignments with human preferences, we further conduct a human evaluation by randomly sampling 100 prompts from the prompt dataset. Similarly, we ask human evaluators to finish the questionnaire used in GPT evaluation. The results are shown in Table 1, which indicates that our method can still achieve the best performance and is consistent with the GPT-4V evaluation results.

4.2. Ablation study

In this section, we show ablation results on the effect of the attention blocks during diffusion generation and the importance of the VLM feedback control in the proposed framework. 50 prompts are randomly sampled from the prompt dataset for all experiments in the ablation study.

Ablation on the attention blocks As we mentioned at the beginning of Section 4, there are three options for the attention blocks used for backward guidance, i.e., near-input blocks, near-middle blocks, and near-output blocks. We empirically found the near-middle blocks can achieve the best control and performance for the generation, which generally contains the richest semantics. Hence here we show the ablation results on different choices of the attention blocks. We utilize SD-v1.4 as the base model, and evaluate the performance of different attention blocks under our framework by GPT-4V. The results are shown in Table 2, which indicates the diffusion generation with near-middle blocks can achieve much better results compared to the other two options.

Ablation on the VLM feedback control The VLM feedback control is a key component in MuLan to provide feedback and adjust the generation process to ensure the every stage’s correct generation. Here, we show the im-

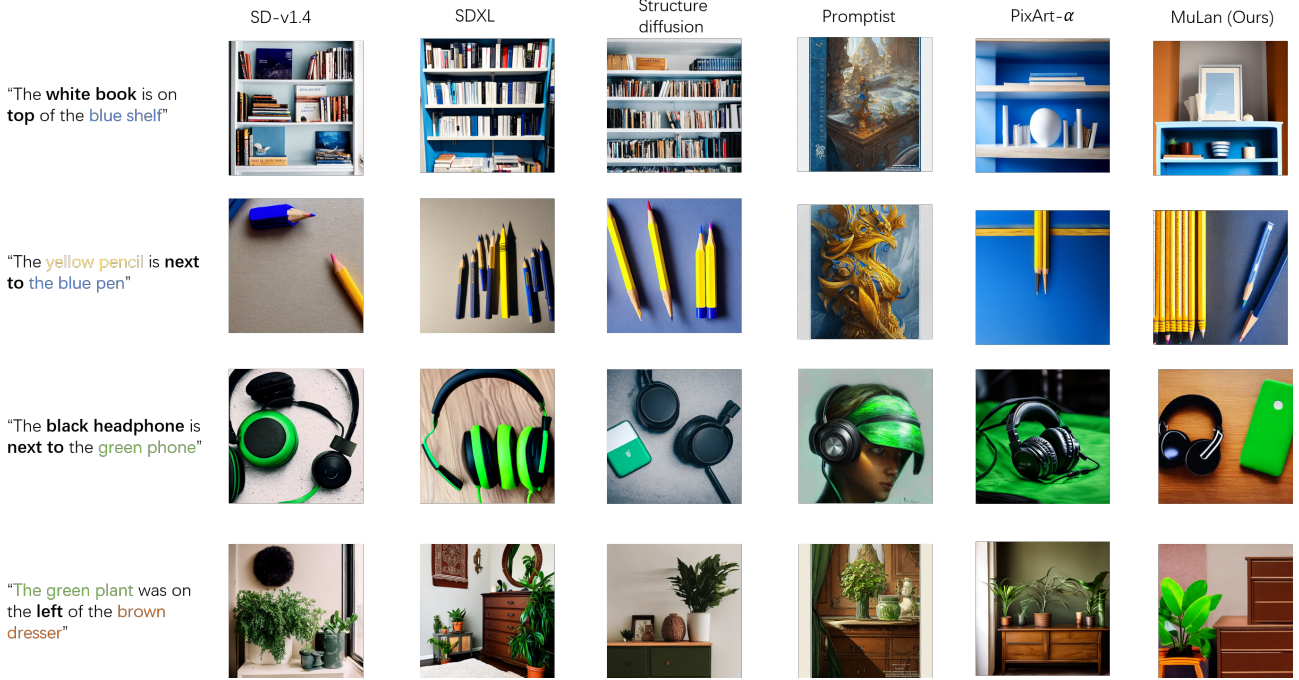


Figure 6. More qualitative examples of images generated by different methods on intricate prompts.

Table 2. Ablation study on attention blocks with SD-v1.4 as the base model. “Objects”, “Attributes”, and “Spatial” denote Object completeness, Attribute bindings, and Spatial relationships. The results (evaluated by GPT-4V (OpenAI, 2023)) show that near-middle attention blocks perform the best for attention guidance.

| Guidance | Objects | Attributes | Spatial | Overall |
|-------------|---------------|---------------|---------------|---------------|
| near-input | 83.67% | 55.10% | 14.29% | 58.37% |
| near-middle | 97.96% | 80.61% | 30.61% | 77.55% |
| near-output | 72.45% | 45.92% | 22.45% | 51.84% |

portance of the feedback by removing feedback control from the whole framework. As shown in Table 3, after removing the VLM, the results would be much worse. It is because there is no guarantee or adaptive adjustment for each generation stage, which verifies that the feedback control provided by the VLM is essential to handle complex prompts. Moreover, we also test MuLan’s compatibility with different VLMs. As shown in Table 4, we compare the Mulan’s performance using different VLMs including LLaVA-1.5 (Liu et al., 2023), GPT-4V (OpenAI, 2023), and Gemini-Pro (Team et al., 2023). The results show that MuLan could still maintain a good performance with different choices of the VLM and achieve good compatibility.

Table 3. Ablation study comparing MuLan with vs. without VLM feedback control, using SD-v1.4 as the diffusion model and GPT-4 as the judge in evaluations. It indicates that feedback control can significantly improve the performance.

| MuLan | Objects | Attributes | Spatial | Overall |
|--------------|---------------|---------------|---------------|---------------|
| w/ Feedback | 97.96% | 80.61% | 30.61% | 77.55% |
| w/o Feedback | 81.63% | 59.18% | 18.37% | 60.00% |

Table 4. Ablation study of the VLM used in MuLan, using SD-v1.4 as the diffusion model and GPT-4 as the judge in evaluations. The results show that the choice of the VLM would not affect the overall performance too much.

| VLM in MuLan | Objects | Attributes | Spatial | Overall |
|--------------------------------|---------|------------|---------|---------|
| LLaVA-1.5 (Liu et al., 2023) | 97.96% | 80.61% | 30.61% | 77.55% |
| GPT-4V (OpenAI, 2023) | 95.92% | 80.61% | 28.57% | 76.33% |
| Gemini-Pro (Team et al., 2023) | 95.92% | 83.67% | 38.78% | 79.59% |

5. Conclusions and Limitations

In this paper, we propose a training-free multimodal-LLM agent (MuLan) to progressively generate objects contained in the complicated input prompt with closed-loop feedback control, achieving better and more precise control on the whole generation process. By first decomposing the complicated prompt into easier sub-tasks, our method takes turns to deal with each object, conditioned on the previous one. The VLM checker further provides a guarantee with feedback control and adaptive adjustment for correct generation at each stage. Extensive experiments demonstrate the superiority of MuLan over previous methods, showing the potential of MuLan as a new paradigm of controllable diffusion generation. However, there are still limitations to be further addressed in the future work. Since the whole generation contains multiple stages, depending on the number of objects, it will take a longer time than a one-stage generation approach. On the other hand, the LLM planner may mistakenly parse the input prompt which results in incorrect decomposition. This could be addressed by first re-writing the input prompt by the LLM to facilitate later processing.

Broader Impact

Our work will bring significant advantages to both the research community focused on diffusion models and the practical application of T2I generation.

In terms of the research community, we present a new and novel controllable image generation paradigm that demonstrates exceptional controllability and produces remarkable results even when tackling challenging tasks. This pioneering approach can offer valuable insights for future investigations into diffusion models.

Regarding industrial applications, our method can be readily employed by T2I generation service providers to enhance the performance of their models. Moreover, the diffusion models operating within our framework are less likely to generate harmful content due to the meticulous control exerted at each generation stage.

References

- Achiam, J., Adler, S., Agarwal, S., Ahmad, L., Akkaya, I., Aleman, F. L., Almeida, D., Altenschmidt, J., Altman, S., Anadkat, S., et al. Gpt-4 technical report. *arXiv preprint arXiv:2303.08774*, 2023.
- Betker, J., Goh, G., Jing, L., Brooks, T., Wang, J., Li, L., Ouyang, L., Zhuang, J., Lee, J., Guo, Y., et al. Improving image generation with better captions. *Computer Science. https://cdn.openai.com/papers/dall-e-3.pdf*, 2(3), 2023.
- Chen, J., Yu, J., Ge, C., Yao, L., Xie, E., Wu, Y., Wang, Z., Kwok, J., Luo, P., Lu, H., et al. Pixart-alpha: Fast training of diffusion transformer for photorealistic text-to-image synthesis. *arXiv preprint arXiv:2310.00426*, 2023.
- Chen, M., Laina, I., and Vedaldi, A. Training-free layout control with cross-attention guidance. In *Proceedings of the IEEE/CVF Winter Conference on Applications of Computer Vision*, pp. 5343–5353, 2024.
- Feng, W., He, X., Fu, T.-J., Jampani, V., Akula, A., Narayana, P., Basu, S., Wang, X. E., and Wang, W. Y. Training-free structured diffusion guidance for compositional text-to-image synthesis. *arXiv preprint arXiv:2212.05032*, 2022.
- Feng, W., Zhu, W., Fu, T.-j., Jampani, V., Akula, A., He, X., Basu, S., Wang, X. E., and Wang, W. Y. Layout-gpt: Compositional visual planning and generation with large language models. *arXiv preprint arXiv:2305.15393*, 2023.
- Hao, Y., Chi, Z., Dong, L., and Wei, F. Optimizing prompts for text-to-image generation. *arXiv preprint arXiv:2212.09611*, 2022.
- Hessel, J., Holtzman, A., Forbes, M., Bras, R. L., and Choi, Y. Clipscore: A reference-free evaluation metric for image captioning. *arXiv preprint arXiv:2104.08718*, 2021.
- Ho, J., Jain, A., and Abbeel, P. Denoising diffusion probabilistic models. *Advances in neural information processing systems*, 33:6840–6851, 2020.
- Huang, K., Sun, K., Xie, E., Li, Z., and Liu, X. T2i-compbench: A comprehensive benchmark for open-world compositional text-to-image generation. *arXiv preprint arXiv:2307.06350*, 2023.
- Li, Y., Liu, H., Wu, Q., Mu, F., Yang, J., Gao, J., Li, C., and Lee, Y. J. Gligen: Open-set grounded text-to-image generation. In *Proceedings of the IEEE/CVF Conference on Computer Vision and Pattern Recognition*, pp. 22511–22521, 2023.
- Lian, L., Li, B., Yala, A., and Darrell, T. Llm-grounded diffusion: Enhancing prompt understanding of text-to-image diffusion models with large language models. *arXiv preprint arXiv:2305.13655*, 2023.
- Liu, H., Li, C., Li, Y., and Lee, Y. J. Improved baselines with visual instruction tuning. *arXiv preprint arXiv:2310.03744*, 2023.
- Nichol, A., Dhariwal, P., Ramesh, A., Shyam, P., Mishkin, P., McGrew, B., Sutskever, I., and Chen, M. Glide: Towards photorealistic image generation and editing with text-guided diffusion models. *arXiv preprint arXiv:2112.10741*, 2021.
- OpenAI. Gpt-4v(ision) system card. 2023.
- Podell, D., English, Z., Lacey, K., Blattmann, A., Dockhorn, T., Müller, J., Penna, J., and Rombach, R. Sdxl: Improving latent diffusion models for high-resolution image synthesis. *arXiv preprint arXiv:2307.01952*, 2023.
- Rombach, R., Blattmann, A., Lorenz, D., Esser, P., and Ommer, B. High-resolution image synthesis with latent diffusion models. In *Proceedings of the IEEE/CVF conference on computer vision and pattern recognition*, pp. 10684–10695, 2022.
- Saharia, C., Chan, W., Saxena, S., Li, L., Whang, J., Denton, E. L., Ghasemipour, K., Gontijo Lopes, R., Karagol Ayan, B., Salimans, T., et al. Photorealistic text-to-image diffusion models with deep language understanding. *Advances in Neural Information Processing Systems*, 35: 36479–36494, 2022.
- Sohl-Dickstein, J., Weiss, E., Maheswaranathan, N., and Ganguli, S. Deep unsupervised learning using nonequilibrium thermodynamics. In *International conference on machine learning*, pp. 2256–2265. PMLR, 2015.

Song, Y., Sohl-Dickstein, J., Kingma, D. P., Kumar, A., Ermon, S., and Poole, B. Score-based generative modeling through stochastic differential equations. *arXiv preprint arXiv:2011.13456*, 2020.

Team, G., Anil, R., Borgeaud, S., Wu, Y., Alayrac, J.-B., Yu, J., Soricut, R., Schalkwyk, J., Dai, A. M., Hauth, A., et al. Gemini: a family of highly capable multimodal models. *arXiv preprint arXiv:2312.11805*, 2023.

A. Detailed prompt template of the global planning by the LLM

As stated in Section 3.3, MuLan first conduct the global planning to decompose the input prompts into N objects before the whole generation process. To this end, given the input prompt p , we prompt the LLM using the following template:

You are an excellent painter. I will give you some descriptions. Your task is to turn the description into a painting. You only need to list the objects in the description by painting order, from left to right, from down to top. Do not list additional information other than the objects mentioned in the description. Description: $\{p\}$.

In this way, the LLM will decompose the input prompt p following the pre-defined order.

B. Detailed prompt template of the local planning by the LLM

As stated in Section 3.4, the LLM is also utilized during the generation stage for local planning of the object's rough position and the object counting.

For the rough position opt_1 planning of the first object, we utilize the following template:

You are an excellent painter. I will give you some descriptions. Your task is to turn the description into a painting. Now given the description: $\{p\}$. If I want to paint the $\{\text{obj}_1\}$ in the painting firstly, where to put the $\{\text{obj}_1\}$? Choose from left, right, top, and bottom. You can make reasonable guesses. Give one answer.

Then the LLM is prompted to figure out the object number based on opt_1 .

If $\text{opt}_1 = \text{left}$, the prompt template for obj_1 is:

You are an excellent painter. I will give you some descriptions. Your task is to turn the description into a painting. Now given the description: $\{p\}$. How many non-overlapping objects are there in the horizontal direction? ONLY give the final number.

If $\text{opt}_1 = \text{bottom}$, the prompt template would be:

You are an excellent painter. I will give you some descriptions. Your task is to turn the description into a painting. Now given the description: $\{p\}$. How many non-overlapping objects are there in the vertical direction? ONLY give the final number.

For the rough position $\text{opt}_n (n \geq 2)$, we utilize the following template:

You are an excellent painter. I will give you some descriptions. Your task is to turn the description into a painting. Now given the description: $\{p\}$. If I already have a painting that contains $\{\{\text{obj}_i\}_{i=1}^{n-1}\}$, what is the position of the $\{\text{obj}_n\}$ relative to the $\{\text{obj}_{n-1}\}$? Choose from left, right, above, bottom, and none of above. You can make reasonable guesses. Give one answer.

Then we prompt the LLM to figure out the object number by:

You are an excellent painter. I will give you some descriptions. Your task is to turn the description into a painting. Now given the description: $\{p\}$. If I already have a painting that contains $\{\{\text{obj}_i\}_{i=1}^{n-1}\}$, how many objects are there in/on the $\{\text{opt}_n\}$ of $\{\text{obj}_{n-1}\}$? Only give the final number.

C. More details on the overlapping processing

Given opt_n and \tilde{M}_{n-1} , the rough mask $M_{n,i}$ can be computed as

$$M_{n,i} = \begin{cases} \left(\tilde{x}_{n-1} \cdot r_i + (\tilde{x}_{n-1} + \tilde{w}_{n-1}) \cdot (1 - r_i), \tilde{y}_{n-1}, \tilde{w}_{n-1} \cdot r_i + \frac{W - \tilde{x}_{n-1} - \tilde{w}_{n-1}}{\text{Num}^n}, \tilde{h}_{n-1} \right), & \text{if } \text{opt}^n = \text{right}, \\ \left(\tilde{x}_{n-1}, \frac{(\text{Num}^{n-1}) \cdot \tilde{y}_{n-1}}{\text{Num}^n}, \tilde{w}_{n-1}, \tilde{h}_{n-1} \cdot r_i + \frac{\tilde{y}_{n-1}}{\text{Num}^n} \right), & \text{if } \text{opt}^n = \text{top}. \end{cases} \quad (8)$$

The illustration for different overlapping ratios is shown in Figure 7.

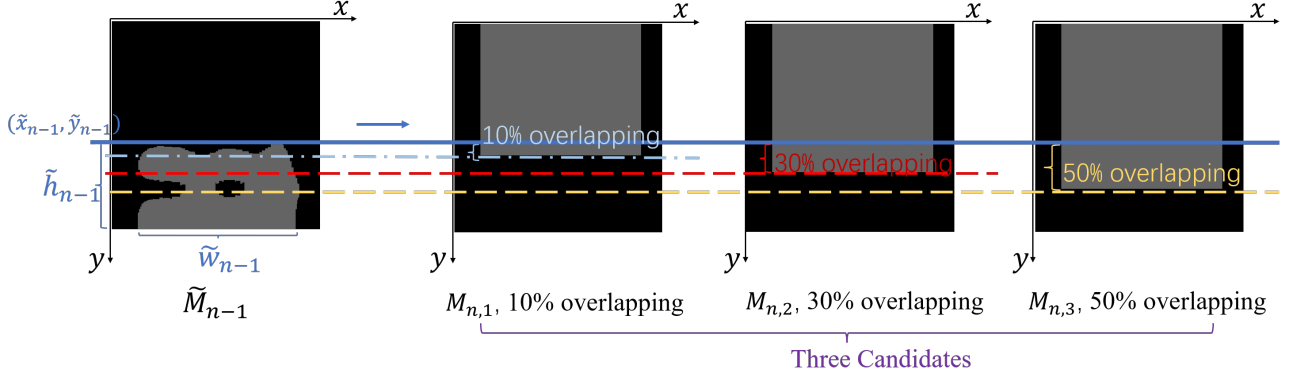


Figure 7. Three candidate masks $M_{n,i}$ of obj_n at position $\text{opt}_n = \text{top}$. They correspond to obj_n overlapping with 10%, 30%, and 50% of obj_{n-1} .

D. More details on the evaluation questionnaire

As shown in Section 4, we design a questionnaire to comprehensively evaluate the alignment between the generated image and the text by GPT-4V (OpenAI, 2023) and human, from three aspects - object completeness, correctness of attribute bindings, and correctness of spatial relationships. Specifically, given an image and a text prompt, for object completeness, we will evaluate if the image contains each single object in the prompt. If the object appears in the image, we will then judge if the attribute bindings of the object in the image align with the corresponding attribute bindings in the text prompt, to evaluate the correctness of attribute bindings. We will also ask GPT-4V or human to judge if the spatial relationships are correct and match the text, as the evaluation of the spatial relationships.

Examples of the questionnaire for different images and text prompts are shown in Figure 8.

E. More qualitative results

We show more examples of different methods in Figure 9.



(a)

Text:
The black chair was on the left of the white table

Questions:

1. Does the image contain the chair? (1 point)
2. Does the image contain the table ? (1 point)
3. If 1 is correct,
is the chair black? (1 point)
4. If 2 is correct,
is the table white? (1 point)
5. If both 1 and 2 are correct,
is the chair on the left of the table ? (1 point.)



(b)

Text:
The green plant was on the right of the white window

Questions:

1. Does the image contain the plant? (1 point)
2. Does the image contain the window ? (1 point)
3. If 1 is correct,
is the plant green? (1 point)
4. If 2 is correct,
is the window white? (1 point)
5. If both 1 and 2 are correct,
is the plant on the right of the window ? (1 point.)

Figure 8. Illustration of the questionnaire for the evaluation of generated images

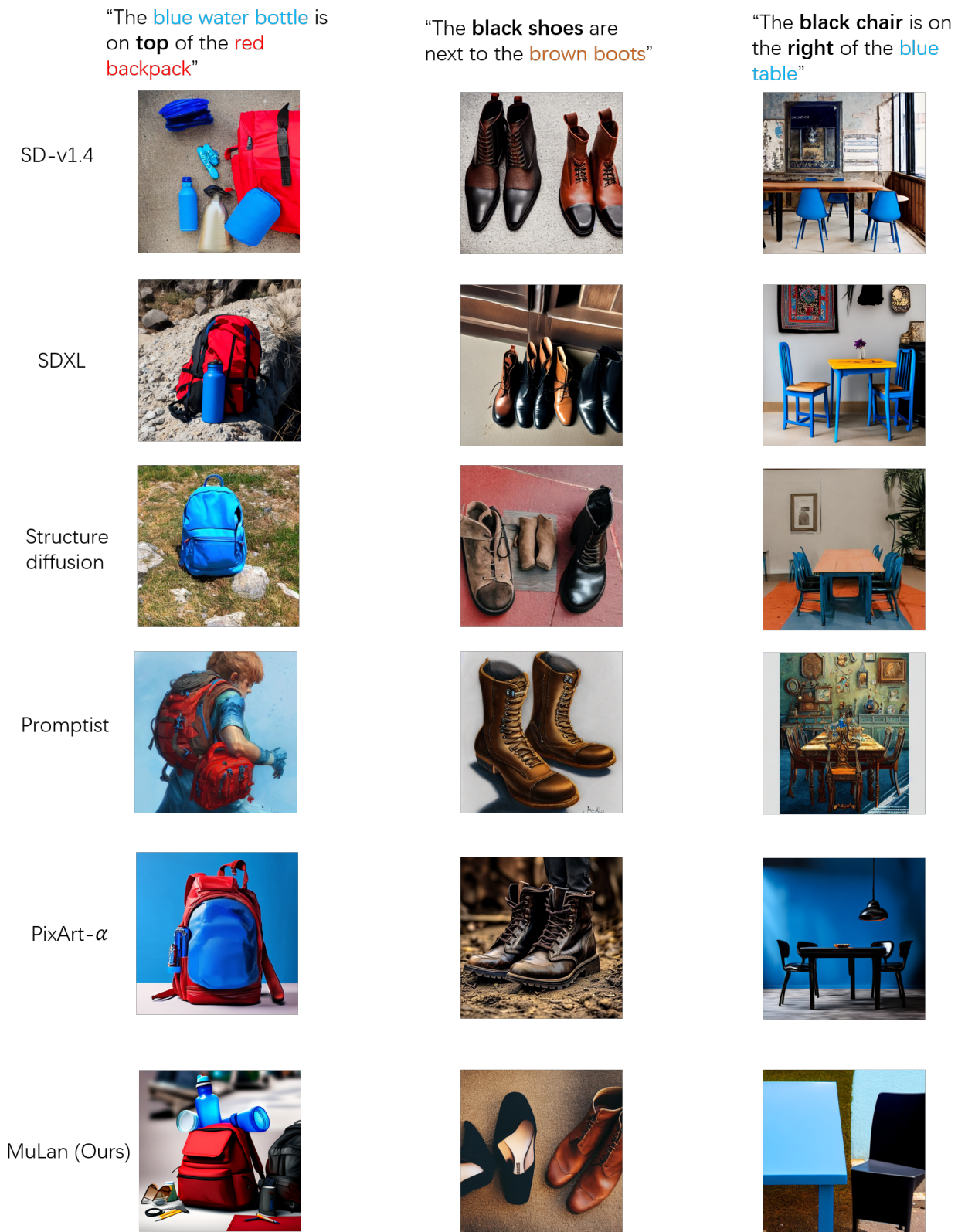


Figure 9. More qualitative examples of images generated by different methods on intricate prompts.